A general bearing deformation model for timber : compression perpendicular to grain

Please check the document version of this publication:

• A submitted manuscript is the version of the article upon submission and before peer-review. There can be important differences between the submitted version and the official published version of record. People interested in the research are advised to contact the author for the final version of the publication, or visit the DOI to the publisher's website.
• The final author version and the galley proof are versions of the publication after peer review.
• The final published version features the final layout of the paper including the volume, issue and page numbers.

[Link to publication](#)

A General Bearing Deformation Model for timber
Compression perpendicular to grain

A.J.M. Leijten [1]

[1] Ass Professor, Dept. of Build Environment,
Eindhoven University of Technology
PO Box 513
5600 MB
 Eindhoven,
The Netherlands
adleijten@gmail.com

Abstract

This study focuses on a new and unique model to determine the elastic bearing deformation of structural timber. Available models that aim to predict the deformation are usually limited in their application. The performance of a simple model is compared to three other models, all being evaluated using experimental test data for the wood species Norway Spruce, Poplar, Beech, Cumaru and Akki and covering eight different load cases. The results show a simple model to have the best performance in deformation prediction and so is a potential candidate for introduction in updated structural timber design codes.

Keywords: timber, bearing, compression perpendicular to grain, deformation.

1 Introduction

In building practice, perpendicular to grain load situations occur in many places. These might be where timber beams (joists) find support, or where studs in timber frames load the bottom and top rail perpendicular to grain. In pre-stressed timber bridge decks, a relatively high pre-stress perpendicular to grain keeps the individual bridge desk laminations together. Currently,

structural timber designers are looking for ways to design higher timber frame houses and even multi-storey mid high-rise buildings, where knowledge about strength and deformation of bearing supports becomes increasingly important. Recently, advances have been made in the development of reliable calculation models for the bearing strength capacity, Leijten [1]. What has to be done is to evaluate bearing deformation models that are easy to apply, accurate and can be used for most bearing situations. The elastic-plastic material behaviour, considering all possible load situations, is hard to predict. This study presents a physical deformation model based on spreading of the bearing stresses which, in a unique way, is able to cover all load cases and is also simple in application and sufficiently accurate for practice. The load cases evaluated are given in Figure 1 where load case A represents the standardized

test piece for the determination of the compression strength and stiffness perpendicular to grain (CPG). Using the stress spreading model proposed by Van der Put [2] and the stiffness data from the standardized test, the deformation of the other load cases can now be derived.
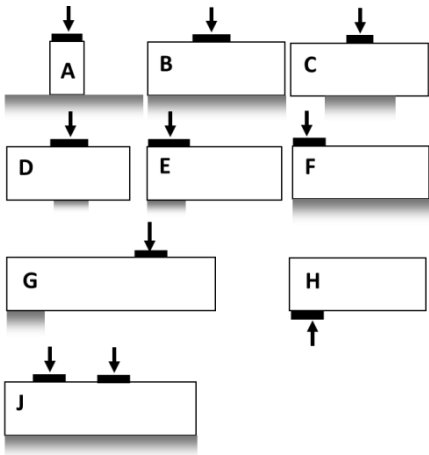

Figure 1 Load cases evaluated in Leijten **[1]**

Although not leading to direct structural failure, CPG deformations can create substantial damage to building components that do not follow the bearing deformation. Knowledge about

shrinkage, the elastic and creep deformation, including mechanic-sorption, are key ingredients for a successful estimation of the total bearing deformation during the life-time of a structure. This article focuses on the evaluation of the bearing deformation which can be characterised by the onset of non- linear behaviour. The elastic deformation forms the starting point for estimation of additional influences like creep.

Not only are deformation models dealing with bearing deformation scars neither of them have yet been accepted by the leading structural timber design codes in the world. This article aims at ending this situation.

2 Bearing deformation models

Deformation models are hard to find in literature. In 1982, Madsen et al. [3] published a bearing deformation model presented in Eq.(1). The model is based on Hook's Law (strain is proportional with the applied stress) as a starting point. The spreading of the bearing stresses was recognised and the total deformation δ is dependent on the depth of the timber beam, h. Further parameters are: the applied load perpendicular to grain $F_{c,90}$, the width of the loaded area b, and a reduced loaded length parallel to grain l_r and l_e, depending on the depth and the distance to the end face, as well as the modulus of elasticity perpendicular to grain E_{90}. The parameters l_r and l_e have, as stated by the author, no physical meaning but are empirical in nature and thus do not relate to the CPG.

$$\delta = \frac{hF_{c,90,d}}{b(l_r + l_e)E_{90}} \tag{1}$$

In the European Design Code of 1987 [4] an empirical model, Eq.(2) is presented but only for the load cases B and F. Hook's Law is again applied but now modified with a factor k_u. It is assumed this factor was determined by evaluation of test results.

$$\delta = k_u \frac{h F_{c,90}}{b l E_{90}}$$

with (2)

$$k_u = \begin{cases} \dfrac{l}{l+2h} & \text{for } a \geq h \\[3mm] \dfrac{l}{l+2h}\left(1+2(1-\dfrac{a}{h})^2\right) & \text{for } a < h \end{cases}$$

The a/h ratio in the modification factor refers to the ratio of the end grain distance a, and the beam depth h. It was F. Mårtensson [5] who proposed another empirical deformation model, Eq (3) that again takes Hook's law as a starting point. The total deformation δ is dependent of the beam depth h, the load $F_{c,90}$, effective loaded area A, and the modulus of elasticity perpendicular to grain E_{90}. The factor μ considers the influence of the depth to bearing length ratio.

$$\delta = \frac{h F_{c,90,d}}{A\left(1+\mu\dfrac{h}{L}\right)E_{90}}$$ (3)

Based on the evaluation of tests and final element calculations, $\mu=0.3$ is proposed. This applies for situations where the loaded area is not too close to the beam end. The author does not specify, however, any specific values for boundary conditions. Furthermore, A. Mårtensson states that deformations caused by creep and mechanic-sorption are believed to be covered by reducing the E_{90}. Gehri [6], mentioned the necessity to use realistic values for the E_{90} and that strength and deformation considerations should not be mixed. Apparently, this model is too limited in its application to be accepted by the timber design codes, as none of the structural timber codes have adopted it. In those days, E_{90} values were taken as a

percentage of the same property parallel to grain and, later in this article, this issue will be elaborated on. Van der Put [2] as well as Blass and Görlacher [7] came up with a deformation model similarly based on Hook's law, but with the assumption of a certain spreading of the bearing stresses in grain direction, combined with the assumption of a linear elastic material behaviour, Eq.(4). The assumption is that the timber outside the stress spreading area does not significantly prevent any bearing deformation. In Eq.(4) the assumed stress spreading gradient is 1:1, the load perpendicular to grain $F_{c,90}$, and the depth and width of the beam are h and b respectively. The length parallel to grain of the loaded area is l, while the support stress length is the effective length, l_{ef}.
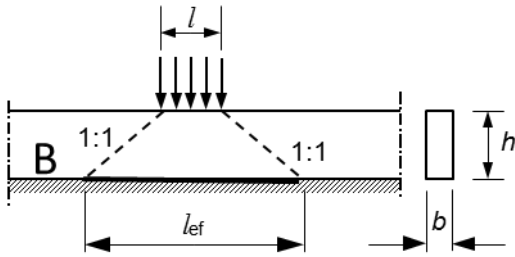

Figure 2. Stress spreading gradient for load case B

$$d\delta = \varepsilon dh = \frac{\sigma dh}{E_{90}} = \frac{F_{c,90}}{b(l+2h)E_{90}}dh$$

$$\delta = \frac{F_{c,90}}{2bE_{90}}\ln\left(1+2\frac{h}{l}\right)$$

(4)

This stress spreading approach can be applied to all load cases. As shown in Figure 3 for load case C the total deformation can be calculated by splitting up the stressed area into two parts. One caused by the top loaded area with loaded length l and depth h_1, and the second caused by the bottom support with loaded length l_s and depth h_2, having an common intersection length indicated by the horizontal dotted line, the so-called effective length l_{ef}. The total deformation is approximated as the summation of the deformation of both stressed areas. Similarly, this

can be applied for close spaced loads and to situations where the loads are close to the end

face, load case F and J, Figure 4. A dotted horizontal line parallel to grain divides the stressed

areas at locations where they start to either interfere with other stressed area or touch the end

face.
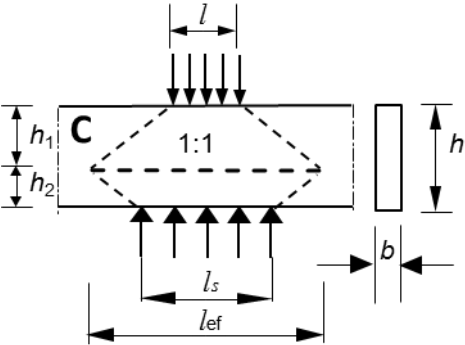
Figure 3. Stress spreading gradient for load case C
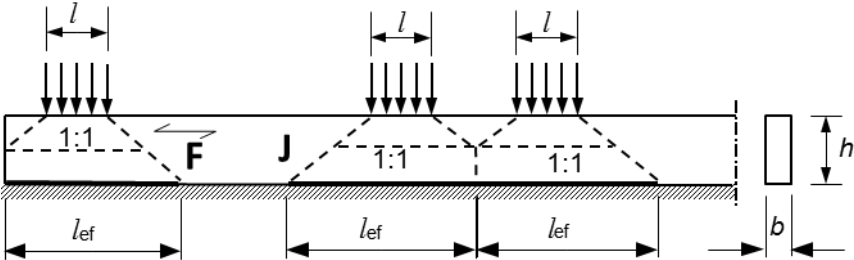
Figure 4. Load cases F and J with interfering stress areas.

The approximated contribution of each stressed area in the total deformation has to be

determined following this procedure.

Taking this linear elastic approach as a starting point, the deformation models associated with

load cases B, C, D, E and F, Figure 1 are listed in the second column of Table 1. For load case

F it is assumed that the load starts at the end face. In Table 1 the model expressions for the

load case J is not given but this one follows from a combination of the other load cases. In

principle, load cases G and H are the same as B because at a certain depth the deformation

perpendicular to grain vanishes, Leijten et al. [8], Figure 5. For these discrete load cases the depth of the beam h is replaced by the effective depth h_{ef} which is equal to 40% of the total beam depth or 140mm, whichever is the smallest. This research result applies to Spruce. For other wood species an FEM analyses can be applied to check the validity of these values. In the equation of Table 1 a factor k is introduced to account for the fact that associated with a stress spreading of 1:1 the deformations are no longer linear elastic but show the onset of yielding. Therefore the approach is taken to modify the modulus of elasticity perp to grain to an apparent value applying kE_{90}.
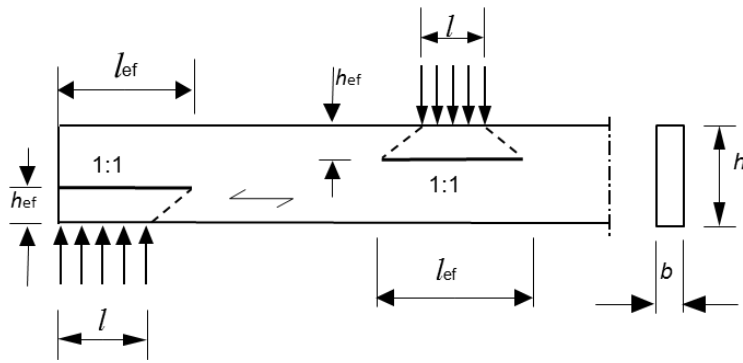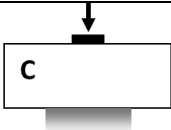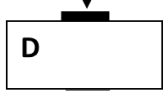
Figure 5. The effective depth for not fully supported load cases

Table 1 Elastic deformation models

Load case	Deformation models based on	
	Eq.(4)	Eq.(5)
B G H	$\dfrac{F_{c,90}}{2bkE_{90}}\ln\left(1+\dfrac{2h}{l}\right)$	$\dfrac{F_{c,90}h}{2bkE_{90}}\left(\dfrac{1}{l}+\dfrac{1}{l_{ef}}\right)$
C	$\dfrac{F_{c,90}}{2bkE_{90}}\ln\left[\left(1+\dfrac{2h_1}{l}\right)\left(1+\dfrac{2h_2}{l_s}\right)\right]$	$\dfrac{F_{c,90}}{2bkE_{90}}\left[h_1\left(\dfrac{1}{l}+\dfrac{1}{l_{ef}}\right)+h_2\left(\dfrac{1}{l_s}+\dfrac{1}{l_{ef}}\right)\right]$
D	$\dfrac{F_{c,90}}{bkE_{90}}\ln\left(1+\dfrac{h}{l}\right)$	$\dfrac{F_{c,90}h}{2bkE_{90}}\left(\dfrac{1}{l}+\dfrac{1}{l_{ef}}\right)$
E	$\dfrac{2F_{c,90}}{bkE_{90}}\ln\left(1+\dfrac{h}{2l}\right)$	$\dfrac{F_{c,90}h}{2bkE_{90}}\left(\dfrac{1}{l}+\dfrac{1}{l_{ef}}\right)$

F	$\dfrac{F_{c,90}}{bkE_{90}}\ln\left(1+\dfrac{h}{l}\right)$	$\dfrac{F_{c,90}h}{2bkE_{90}}\left(\dfrac{1}{l}+\dfrac{1}{l_{ef}}\right)$

A different formulation using the same starting point of stress spreading is based on the following. Calculate the average stress perpendicular to grain taken at the loaded area and the support area and apply Hook's law as follows:

$$\sigma_{avg}=\frac{F_{c,90}}{2b}\left(\frac{1}{l}+\frac{1}{l_{ef}}\right)$$

$$\delta=\varepsilon h=\frac{\sigma_{avg}h}{kE_{90}}=\frac{F_{c,90}h}{2bkE_{90}}\left(\frac{1}{l}+\frac{1}{l_{ef}}\right)$$

(5)

In Eq.(5) the depth h can either be the full depth of the beam as in load cases B and F, or the so-called effective depth h_{ef} in load cases C, G and H. For load case C, for instance, Figure 3 both stressed areas with depth h_1 and h_2 contribute to the total deformation as mentioned earlier. The location where both stresses meet and have equal length parallel to grain is called the effective length l_{ef} which can be calculated with Eq.(6) where the length of both loaded areas are l and l_s.

$$l_{ef}=h+\frac{l+l_s}{2}$$

(6)

This method of adding deformations of separate stress fields is also easy to apply to more complex load cases such as F and J, Figure 4. Also, when the stress field boundaries interfere with a neighbouring stress field or by the end grain face, the contribution to the total deformation can be calculated separately by following this principle. The horizontal dotted lines in Figure 4 separate the individual stress fields. A general expression for the model of Eq.(5) accounting for a number of stress fields n can be written as Eq.(7).

8

$$\delta = \frac{F_{c,90}}{2bkE_{90}} \sum_{n=1}^{n} h_n \left(\frac{1}{l_n} + \frac{1}{l_{n+1}} \right)$$ (7)

where

δ is the total bearing deformation,

$F_{c,90}$ is the load perpendicular to grain,

b the width of the loaded area,

k modification factor to change E_{90} into an apparent value

E_{90} is the modulus of elasticity of the wood species involved perpendicular to grain,

n are the number of stress fields,

h_n the distance between the loaded and the bearing area of each individual stress field,

l_n, l_{n+1} the loaded length of the loaded area, n and bearing area, $n+1$.

The appropriate expressions for load cases B, C, D, E and F are given in the right column of Table 1. Comparing the expressions in the two columns, it will be clear that the equations in the right column do not change by load case and this eases the use for the design engineer. An evaluation of test data and further analyses are required to see which of the models perform most successfully and with satisfactory accuracy.

3 Test Data

The wood species involved in the evaluation are Norway Spruce, Poplar, Beech, Cumaru and Akki (Azobé), with average wood densities of 418kg/m^3, 433kg/m^3, 623kg/m^3, 947 kg/m^3 and 1163 kg/m^3 respectively. All test specimens were conditioned at 60% RH and 20^{0}C. The experimental determination of the E_{90} is a key parameter to evaluate the models. This material property should be determined in a standardized and physically correct way. In Leijten and Jorissen [9], it is shown that the prescribed test specimens in the tests standards of North America and Australia/New Zealand are unsuitable for this purpose. Only in CEN/EN408

9

[10] a cubic type test piece is prescribed that is loaded over the full surface area and as such provide physically more correct values than the partly loaded test specimens of the other standards. The dimensions of this test specimen $bxhxl$ are 45x90x70mm, with the width b, depth h and parallel to grain length l, respectively. During the test, the total deformation together with the applied load results in a load-deformation curve, Figure 6, left.

The compressive strength $F_{c,90}$, is defined by the intersection of a line parallel to the linear elastic part of the load-deformation curve, off-set by 1% of the specimen depth. This straight line is used to calculate the modulus of elasticity of the standard test specimen, E_{90}. If the value of E_{90} is used to determine the deformation at the defined $F_{c,90}$, this value has to be reduced which leads to the introduction of an apparent modulus of elasticity, kE_{90} as mentioned earlier.
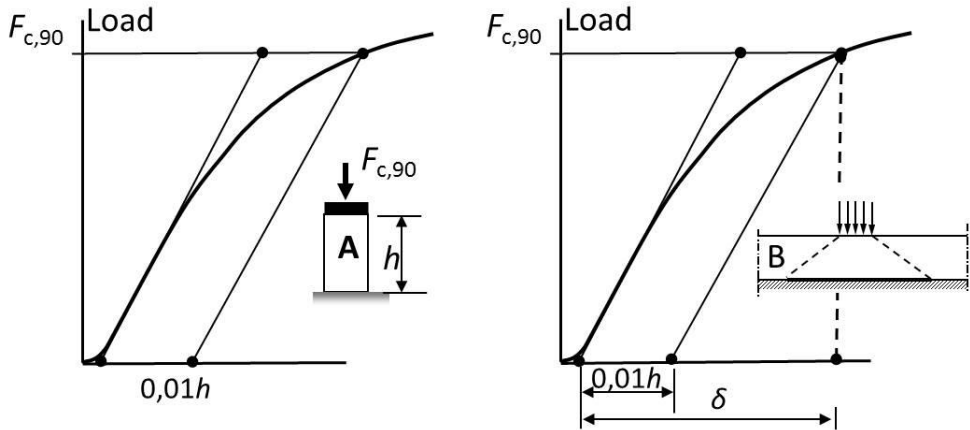
Figure 6. Test according to EN408, load case A (left) and a test results for load case B (right).

A typical experimentally determined load-deformation curve for load case B is given in Figure 6, right. The determination of the CPG strength follows the same procedure as for the standard test piece, but now the off-set line is 1% of the full beam depth for load case B, or 1% of the effective beam depth dependent on the individual load case. The deformation associated with this CPG strength is δ, as is given in the figure which does not include any delayed load uptake at the beginning of the load application. This deformation is recorded and

is later compared with the model predictions. Due to the non-linearity, the experimentally determined displacement δ may be somewhat greater than that which the models predict as they assume linear elastic response. It may be expected, therefore, that model predictions are conservative. In this respect, it is time to address a shortcoming of the standard test procedure of EN408 that affects the determination of the modulus of elasticity perpendicular to grain. It might seem logical to take as deformation the total deformation (over the full depth) of the standard test piece and similarly measure the total deformation of any other test piece. However, the gauge length to record the deformation currently prescribed by EN408 is set to 60% of the specimen depth. This results in the undesirable effect shown in Figure 7 for load case B, where the highest deformed zone is omitted from the observation. Models to predict the deformation aim at predicting the total deformation. For this reason, it is important to analyse experimental results as to what gauge length is used.

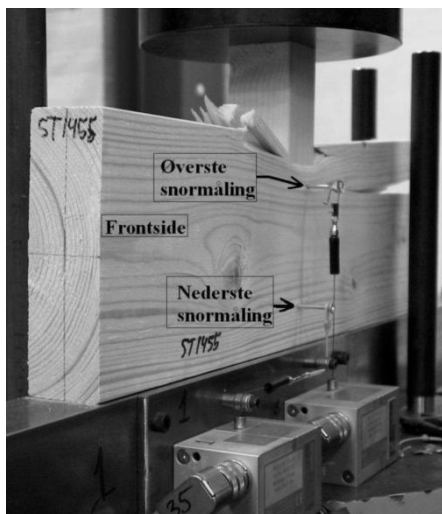Figure 7. Load case B measuring the deformation over 60% of the test specimen depth, Hansen [11]. Arrows point at the attachment points of the transducer.

Bodig and Jayne [12] showed that CPG deformation and failure is initiated by weak annual rings. When they are located outside the gauge length, the recorded deformation is unreliable as observed by Levé et al. [13]. To support the suggestion of taking the full test specimen

11

depth as gauge length instead of 60% of the depth, investigations by Hansen [11] are presented. The wood species used was Norway Spruce with an average moisture content of 12%. Hansen [11] uses both gauge lengths simultaneously, from which the modulus of elasticity E_{90}, is derived taking the linear part of the recorded load-deformation curve. At first, the standard EN408 test piece of 90mm depth is taken and deformations recorded. Similar tests are performed with test pieces of 145mm and 220mm depth with 10 replicates each. The first column of Table 2 shows the specimen depth while subsequent columns show the mean E_{90}, and the coefficient of variation for each gauge length. The coefficient of variation of E_{90} for the 90 mm standard specimens (EN408), is only one third of the coefficient of variation taking the 60% gauge length. Increasing the test specimen depth from 90 to 145mm and 220mm does not affect the E_{90} value when taking the full depth. This is in contrast to when the 60% gauge length is taken as the 60% gauge length delivers consistently higher values for the variation coefficient. In another part of his research, Hansen [11] also performed tests for load case B, Figure 7.

Table 2. Overview of E_{90} test results by Hansen [11] for load case A specimens, Spruce.

n=10	E_{90} gauge length total depth	Var. coeff.	E_{90} *gauge* length 60% of total depth	Var. coeff.
Depth [mm]	mean [N/mm^2]	[%]	mean [N/mm^2]	[%]
h=95	199.3	9	199.3	31
h=145	211.2	43	240	96
h=220	203.2	29	305.9	48
Mean	204		248	

He varied the specimen depth again from 95mm, 145mm to 220mm as well as varying the loaded length parallel to grain from 45mm, 95mm to 145mm. The specimen width was kept constant and the number of replicates per test series was five. Results are presented in Table 3. Comparing the mean E_{90} values, as well as coefficient of variation of both tests, again support the earlier findings that taking the total test specimen depth culminates in more

reliable test results. For this reason, all deformations used to evaluate the deformation models are determined using the full specimen depth as gauge length.

Table 3. Overview of E_{90} test results by Hanssen [11] for load case B specimens, Spruce.

n=5	loaded length	E_{90} gauge length total depth	Coeff of var.	E_{90} gauge length 60% of total depth	Coeff. of var.
Depth [mm]	[mm]	mean [N/mm^2]	[%]	mean [N/mm^2]	[%]
h=95	45	398	3	337	21
	95	268	13	240	10
	145	191	8	233	40
h=145	45	601	16	949	51
	95	403	19	769	86
	145	304	32	353	58
h=220	45	706	14	1441	40
	95	463	25	965	49
	145	337	7	502	27

In Table 4, an overview is presented of the modulus of elasticity E_{90} of the standard test specimens, tested in accordance with EN408 for all the wood species involved in this study (taking the full specimen depth as gauge length). In building practice, the structural design engineer will usually take the strength and stiffness values from a particular strength class system. For the wood species involved these values have been added in the last column. For Spruce the material was CE marked C24 while for Poplar a value was taken from strength class C27 based on a mean density of 433kg/m^3. In strength classes the material properties are given independent of the annual ring orientation. For this reason the annual ring orientation is not addressed in the test method of EN408 and taken at random.

Table 4. Overview of E_{90} values, load case A, EN408

Wood species	Sample number	Number of tests	Mean E_{90}		Strength class
			[N/mm^2]	CV [%]	Value EN338
	1	25	150	39	
Spruce	2	13	141	55	
	3	14	180	39	
	4	10	170	44	

Mean			158	48	370
Poplar	1	31	183	32	
	2	12	116	11	
	3	10	236	40	
mean			159	32	380
Beech	1	10	976	25	700
Cumaru	1	12	911	8	1240
Akki	1	9	1082	33	1810

For the European situation, the strength classes are specified in EN 338 [14]. Due to a lack of knowledge when the strength class values were initially set, E_{90} was taken as $E_0/30$ for softwood and $E_{90}=E_0/15$ for hardwood. Table 4 shows a considerable deviation for Norway Spruce between the observed test value of 158N/mm^2 and the strength class value of 370N/mm^2. For Poplar the differences are 159N/mm^2 and 380N/mm^2 respectively. In both cases the recorded modulus of elasticity E_{90} is approximately 50% of the E_{90} value. In his elaborate study, Hübner [15] p. 49 reports a mean value for Beech of 1040N/mm^2 which is close to value of 976N/mm^2 in Table 4. However, based on the mean density of 629kg/m^3 the strength class value is D27 where E_{90} is 700N/mm^2. For the other tropical hardwood species, Cumaru and Akki a similar approach was taken, strength classes D65 and D80, respectively. Apparently, there are reasons to question the moduli of elasticity perp to grain by the strength class system of EN 338.

4 The test data base for the load cases B to J

Specimens of Spruce, Poplar, Beech, Akki and Cumaru are cut from planks that vary in size suitable to test all the load configurations of Figure 1. Besides the data base which contains all the test results carried out at TU-Eindhoven, a limited number of test data from literature could be added. An overview of the variation in dimensions of the tested pieces, mainly sawn timber, is presented in Table 5 for the respective load cases. Only in the case of Norway Spruce is a distinction made between structural timbers (ST) and glued laminated timbers (GLT). The table also includes standard test specimen dimensions, in accordance with

standards like ASTM- D143, AZ/NZ and ISO 13910. For load case J, the spacing between the

load areas and the distance to the end face have been varied from 30mm to three times the

specimen depth 3h.

Table 5. Overview of test specimens evaluated for the bearing models.

Load case	Wood species*	No of samples	No of tests	Width	Total specimen depth	Effective depth	Loaded length
		#	#	[mm]	[mm]	[mm]	[mm]
B [11] [16] [17]	Spruce ST	15	124	45-90-51-108-150-160	45-90-95-145-150-200-220	See total depth	45-50-95-145
	Spruce GLT	10	138	90-160	200-405-480		90-150
	Poplar	6	36	45-95-150	45-80-150		45
	Akki	4	17	45-95-145	45-95-145		50
	Cumaru	1	12	51	51		51
Total		36	327				
C	Spruce ST	1	8	39	219	92-126	100-150
	Akki	4	14	45-95-195	45-95-195		50
Total		5	22				
D	Spruce ST	2	33	35-39-90	40-45-90	20-23-45	48-50-90
	Spruce GLT	1	11	90	90	45	48
	Poplar	6	38	45-80-150	45-150	23-40-75	45
	Akki	4	18	45-95-195	45-195	23-98	50
	Cumaru	1	12	35	45	22,5	90
Total		14	112				
E	Spruce ST	3	30	45-48	45-90-150	23-45-75	45-48
	Spruce GLT	1	8	90	90	45	48
	Poplar	6	37	45-80	45-80-150	23-45-75	45
	Akki	4	13	45-95-195	45-95-195	23-48-98	50
Total		14	88				
F	Spruce GLT	6	159	150	200-480	See total depth	150
	Akki	4	21	45-95-195	45-95-195		50
Total		10	180				
G	Spruce ST	14	106	40-48-80-90	219	88	50
H	Spruce ST	4	51	48	198	79	48
	Spruce GLT	1	6	90	405	140	90
Total		19	163				
J	Spruce ST	14	120	45-75-90	45-90-150-280	See total depth	45-50
	Poplar	6	40	45-80	45-80-150		45
	Beech	6	41	53-90	70-90		45
	Akki	6	31	45-95-195	45-95-195		50
Total		26	232				

* ST – Structural timber, GLT – Glued Laminated Timber

The total number of tests performed, including tests reported by Hansen [11], Moseng and

Hagle [16] and Augustin and Schickhofer [17], are presented in Table 6. The number of tests

for Cumaru is limited, covering only load case B and D with 12 results each. However, the

deformation test results are in line with the range that is found for the other wood species and load cases.

Table 6. Number tests per wood species

Wood species	Number of tests
Spruce	794
Poplar	191
Beech	41
Akki/Azobé	114
Cumaru	24
Total number	1164
Total number of samples	134

5 Model Evaluation

The models and the test data have been presented. In the following, the ability of the models to predict the experimentally determined bearing deformation is investigated. The models given by Eq.(1) and (3) will be left out of the evaluation either because they do not distinguish between load cases or they contain unknown parameters. The models that will be evaluated are presented in Eq.(2), Eq.(4), Eq.(5) for as far the load cases apply. The models require an input value for the modulus of elasticity E_{90}, which is taken from Table 4.
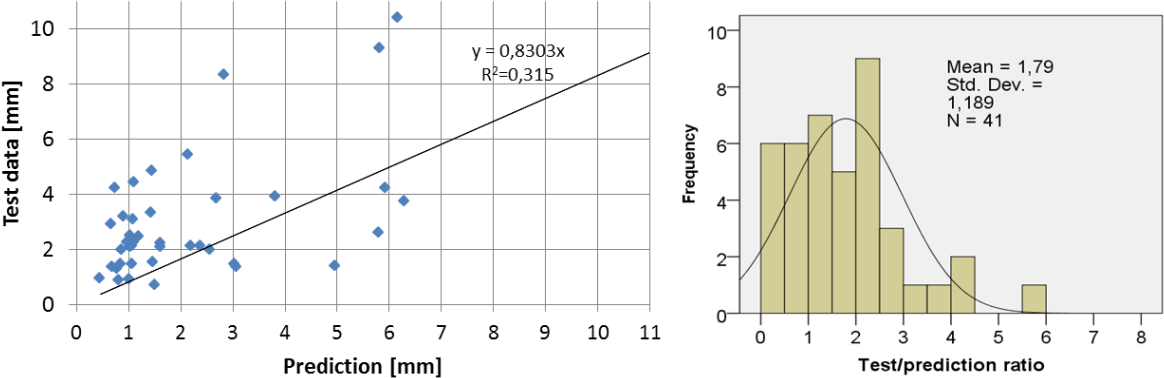

Figure 8. Model Eq.(2) versus test data of Spruce.

The test results are now presented in a graphical way to allow a quick visual assessment. In Figure 8 test results versus the model predictions using model Eq.(2) are presented for Norway Spruce only covering load cases B and F. Every dot in the graph represents the mean

value of a sample. It represents 476 test results from 41 samples. To visualise the a-symmetry of the results, the ratio between the observed deformation and the model predictions are calculated and presented by a histogram. The visual scatter of the data is high as represented by the high frequency of values over a considerable range for the test/prediction ratio on the horizontal axes. The histogram is completed by a fitted to the data normalised distribution of which the mean and standard deviation is given. It shows that the model mainly underestimates the recorded displacements. The coefficient of determination $R^2 = 0,315$ indicates that only about 32% of the variation can be explained by the model.
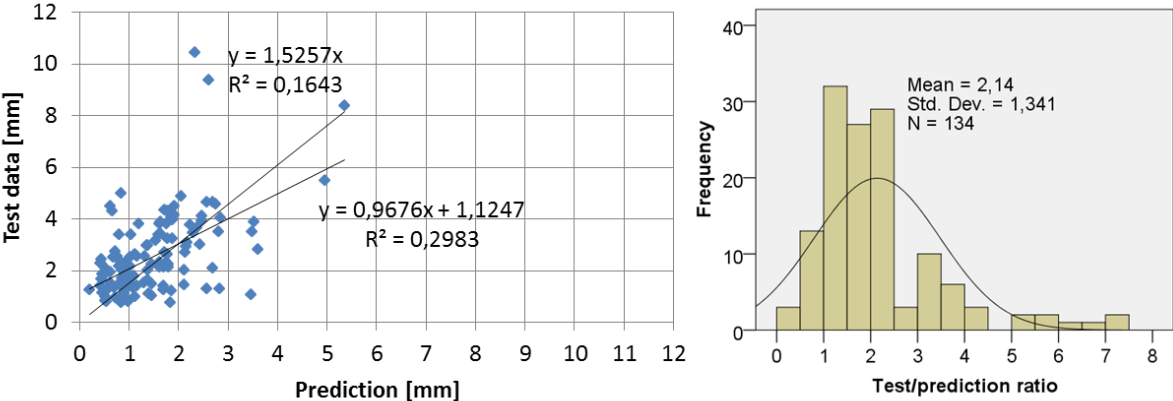

Figure 9. Model Eq.(4) versus test data; all wood species.

In the same way the model of Eq.(4) is evaluated in Figure 9, all the test data related to the wood species Norway Spruce, Poplar, Cumaru and Akki covering load cases B, D and H are evaluated. The number of samples is 134, representing 481 test results. Two trend lines are shown. One where the intersection with the origin is forced y=1.53x and one where the intersection with the vertical axes is left free y=0.97x+1.12. As expected this affects the coefficient of determination, $R^2 = 0.16$ and $R^2 = 0.298$, respectively but in any case both are low. The histogram shows a mean test to model prediction ratio of 2.15 which is still far from the ideal 1.0.

The performance of the model of Eq.(5) is shown in Figure 10 for the wood species Spruce only. The number of samples is 72, representing 794 test results covering for all load cases.

17

As in Figure 9 again the two trend lines are shown. Compared to the previous models, the trend line runs more diagonally y=1.009x with a coefficient of determination of R^2=0,57 which increases to 0.67 when the intersection with the origin is left free. The histogram is quite different from the previous histograms in Figures 8 and 9. The mean of the fitted normalised distribution with a mean of 1.24 and a standard deviation of 0.51 is much better than the model of Eq.(4). How the model of Eq.(5) performs considering the results of the
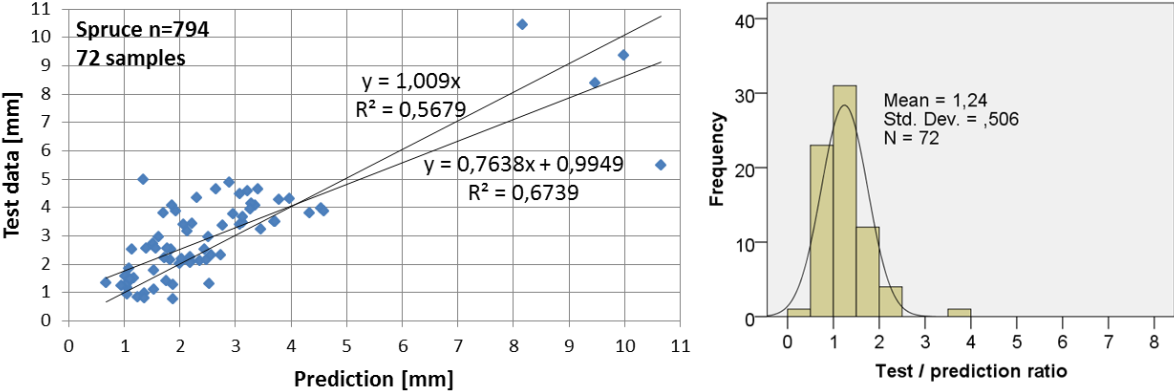
Figure 10. Model prediction Eq.(5) versus test data for Spruce.

deciduous wood specimens is presented in Figure 11 with 62 samples, representing 370 test results. The result in terms of the coefficient of determination is less than in Figure 10 for Spruce only. The fitted normalised distribution in the histogram shows that the mean and standard deviations are close with Figure 10 values and still better than the results with the previous models shown in Figure 8 and 9.
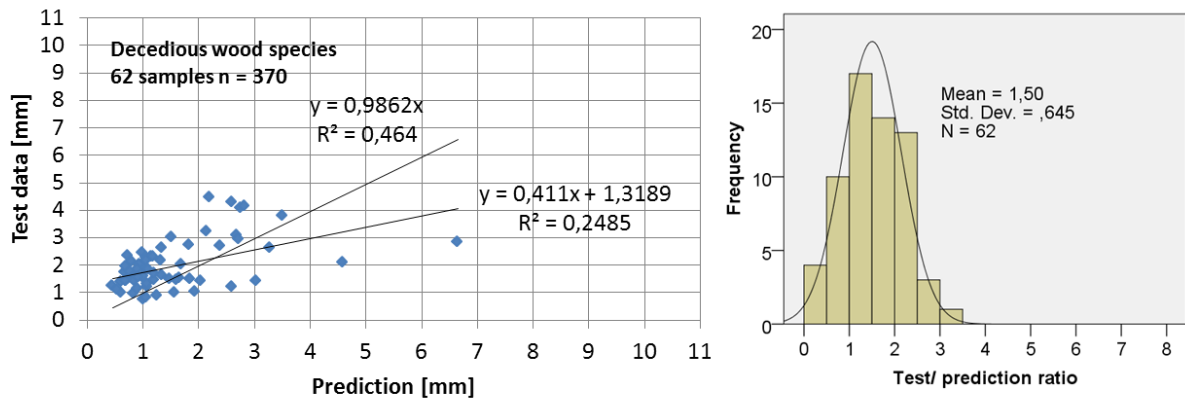
Figure 11. Model prediction Eq.(5) versus test data of deciduous wood species.

Merging the test data of Figure 10 and 11 results in Figure 12. This represents all wood species and all load cases with a total of 134 samples, comprising 1164 test results altogether. This performance is the better one in comparison with the other models. The coefficient of determination R^2 of the two trend lines are 0.46 when the intersection with the origin is forced, and 0.62 when left free. The performance of Model Eq.(5), in terms of mean and standard deviation of the fitted normalised distribution, is 1.36 and 0.587. This is considerably better than previous models Eq.(2 and 4) as shown in Figures 8 and 9.
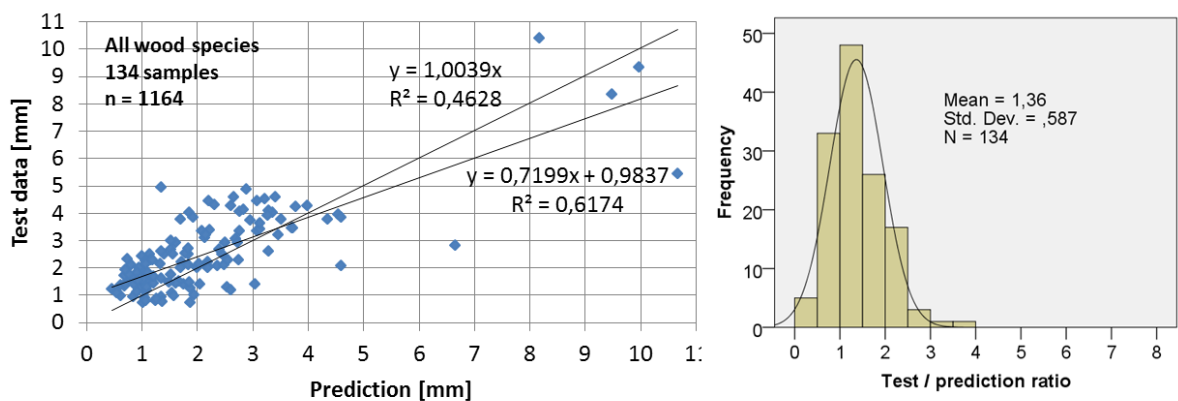

Figure 11. Model Eq.(5) versus test data.

To discover if the model results are influenced by depth of the specimens, the test value to model Eq.(5) prediction ratio is set against the specimen depth or where appropriate the

effective depth, Figure 13. The trend line indicates that the model results are consistent, and the increasing specimen depth hardly affects the outcome. Presumably, this is affected by the limited number of experimental results with fully supported glued laminated specimens of 480mm depth. Figure 13 shows that the majority of tests were performed on timber specimens with a depth smaller than 200mm. It should be considered, however, that the test data base also comprises results with glued laminated specimens of 600mm depth but loaded at discrete locations, Figure 5. For these cases, the effective depth is a maximum of 140mm. To gain more insight into the depth effect, more research should be performed. Whatever load case is considered, the CPG spreading stresses, as indicated in Figure 3 and 4, could disconnect for large specimen depth and show that they can be considered as discrete loading areas as given in Figure 5.
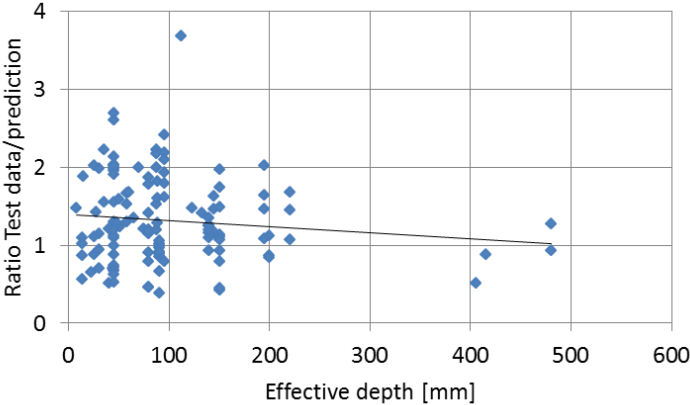

Figure 13 The effect of the effective depth with Eq.(5)

What has not yet been discussed is the necessity of the modification factor k that was introduced to modify the modulus of elasticity E90 to an apparent value in order to cater for any non-linearity. The results shown in the figures above were obtained with $k=1.0$. Some trials changing this value did not show any improvement of fit, so no adjustments are proposed.

6 Serviceability deformation

The models aspired to predict the deformation at the point where the standard CPG strength is attained, Leijten[1]. For practical application the deformations at the serviceability limit will also be of interest for the structural designer. Is it possible to adapt the model and to predict the deformation at serviceability limit? For this reason the test data of several load cases and test series were reviewed. In general, the deformation at serviceability limit appeared to be approximately 50% of the deformation attained for the CPG strength. For practice, it simply means that Eq.(5) can be maintained with two adaptions. The E_{90} is doubled and the load perpendicular to grain is changed to the serviceability load, $F_{c,90,ser}$ as given in Eq.(8).

$$\delta = \frac{F_{c,90,ser}}{4bE_{90}} \sum_{n=1}^{n} h_n \left(\frac{1}{l_n} + \frac{1}{l_{n+1}} \right) \tag{8}$$

How realistic the deformation predictions for building practice turn out to be cannot be seen separately from the accuracy of the strength class E_{90} values and the way they are determined by using a standard test method. As mentioned, the values for Norway Spruce in EN338 are twice as high as determined experimentally, leading to design calculations that underestimate the actual behaviour.

7 Conclusion

The aim of the study is to investigate the ability of models to predict the bearing deformation of timber loaded perpendicular to the grain. Starting point for the deformation models is the accurate determination of the modulus of elasticity perpendicular to grain for the wood species tested. The test standard EN408 allows assessing the physically correct value by using a prismatic test loaded over the full surface. Unlike the method prescribed by this standard the deformations should be taken over the total specimen depth to obtain realistic values. For this reason revision of this part of EN408 is advised. The strength class values in EN338 for the modulus of elasticity perpendicular to grain are questionable and should be re-evaluated.

The modification factor k that was introduced to modify the modulus of elasticity E_{90} to an apparent value does not improve the model fit and subsequently can be taken as 1.0 in the models. The best performing model is given by Eq.(5). Regarding the evaluation of this bearing model for Spruce a satisfactory fit was obtain. This data base consisted of 72 samples, representing 794 test results covering for all load cases. In Figure 9 the trend line characteristics are given as y=1.009x with a coefficient of determination of R^2=0,57 which increases to 0.67 when the intersection with the origin is left free. When the whole test data base is used, covering the wood species Spruce, Beech, Poplar, Cumaru and Akki, comprising of 134 samples and 1164 test results these trend line values change to y=1.004x with a coefficient of determination of R^2=0,46 and 0.62, respectively.

The bearing deformation model of Eq.(5) is therefore the preferred model regarding the simplicity (ease of use) and the predictive ability compared to the other models. It is the only model ever reported that can be applied to all the practical load cases and with this accuracy.

References

[1] Leijten A.J.M., "The bearing strength capacity perpendicular to grain of Norway Spruce - Evaluation of three structural design models," *Construction and Building Materials,* vol. 105, p. 8, 2016.

[2] Put van der TACM, "Restoration of exact design for partial compression perpendicular to grain," *Wood Material Science and Engineering,* vol. 7, no. 4, pp. 225-236, 2011.

[3] Madsen B, Hooley RF, Hall P, "A design method for bearing stresses in wood," *Canadian Journal of Civil Engineering,* vol. 9, no. 2, pp. 338-349, 1982.

[4] Eurocode No5: Common unified rules for timber structures, Brussels: Commission of the European Communities, 1987.

[5] Mårtensson A, "Short- and Long term Deformations of Timber Structures," in *Timber Engineering*, John Wiley & Sons, LTD, 2003, p. 18.

[6] Gehri E, "Timber in compression perpendicular to grain," in *IUFRO*, Copenhagen, 1997.

[7] Blass H J and Goerlacher R, "Compression perpendicular to grain," in *Proceedings of the 8th World Conference on Timber Engineering*, Lahti, Finland, 2004.

[8] Leijten AJM;Jorissen AJM; de Leijer BJC, "The local bearing capacity perpendicular to grain of structural timber elements," *Construction and Building materials,* vol. 27, pp. 54-59, 2012.

[9] Leijten AJM and Jorissen AJM, "Global test standards and global design rules for compressive strength perpendicular to grain, p393-400," in *11th World Conference on Timber Engineering*, Reva del Garda, Trentino, Italy, 2010.

[10] CEN-EN408 Timber Structures, Determination of some physical and mechanical properties, Brussels: European Comite of Standization, 2009, p. 38.

[11] Hansen F, "Konstruktionstrae Trykbelastet Vingelret Pa Fiber Retningen," DET-Teknisk naturvidenskabelige fakutet Aalborg University Demark, Aalborg, 2005.

[12] Bodig J. and Jayne B.A., "Mechanics of wood and wood composites," Van Nostrand Reinhold Company, New York, 1982.

[13] Levé le C; Maderebner R; Flach M, "Compression strength and stiffness perpendicular to the grain - Influences of the material properties, the loading situation and the gauge length," in *INTER paper 47-6-1*, Bath UK , 2014.

[14] CEN-EN 338 , "Structural timber - Strength classes," CEN, Brussel, 2015.

[15] Hübner U., "Mechanische Kenngrößen von Buchen- Eschen- und Robinienholz für Lastabtragende Bauteile," Verlag der Technischen Universität Graz, Graz, Austria, 2013.

[16] Moseng M;Hagle D, "The capacity of wood for compression perpendicular to the grain," Institut for matematiske realfag og teknologi NMBU, Oslo, Norway, 2012.

[17] Augustin M;Schickhofer G, "Behavior of glulam in compression perpendicular to grain in different strength grades and load configurations," in *CIB-W18 paper 39-12-5*, Florence, 2006.